The Tertiary Structure of the Hairpin Ribozyme Is Formed through a Slow Conformational Search†

Goran Pljevaljčić,‡ Dagmar Klostermeier,‡,§ and David P. Millar*

Department of Molecular Biology, The Scripps Research Institute, La Jolla, California 92037

Received October 18, 2004; Revised Manuscript Received January 16, 2005

ABSTRACT: The hairpin ribozyme is a small catalytic RNA comprised of two internal loops carried on two adjacent arms of a four-way helical junction (4WJ). To achieve catalytic activity, the ribozyme folds into a compact conformation that facilitates the formation of tertiary interactions between the two loops. We have investigated the folding kinetics of the natural 4WJ form of the hairpin ribozyme, as well as a minimal construct consisting of just the two loop-containing duplexes, by means of stopped-flow fluorescence resonance energy transfer between donor and acceptor probes attached to the ends of the loop-bearing arms. Folding was initiated by the addition of Mg^{2+} ions or a pseudosubstrate strand to the ribozyme, and the ensuing changes in the emission of both donor and acceptor were monitored over time. Both ribozyme constructs exhibited slow, biphasic kinetic behavior, attributed to two parallel folding pathways leading to compact, docked structures. Two distinct folding rates were observed across a range of Mg^{2+} concentrations, and increasing amounts of Mg^{2+} accelerated both rates. Notably, both rates were essentially independent of temperature, indicating that the corresponding activation enthalpies were negligible, in contrast to the large activation enthalpies generally observed for RNA folding processes. Instead, the slow folding was due to unfavorable entropy changes in reaching the transition state, indicating that the ribozyme tertiary structure forms through a slow conformational search. These features were observed in both forms of the ribozyme, indicating that the conformational search is confined to the two loop regions and is largely independent of the overall ribozyme architecture. Conformational search may be a general mechanism of tertiary structure formation in RNA.

To perform their diverse range of biological functions, RNA molecules must fold into unique three-dimensional structures that create catalytic centers or specific ligand recognition sites. The mechanisms by which RNA chains fold into specific tertiary structures are just beginning to emerge and are the subject of much current interest (reviewed in refs *1*−*3*). While fast folding is sometimes observed, the tertiary folding of RNA is usually very slow, particularly for large RNA molecules with complex tertiary structures. Generally, the folding of large RNAs can be separated into distinguishable early and late events. Early events correspond to the rapid nonspecific collapse of the RNA chain into compact structures with little native tertiary structure (*4*−*6*). In later steps of folding, these collapsed structures rearrange through a slow conformational search to form the native tertiary structure. Additionally, many RNAs populate non-native secondary and tertiary structures during the course of folding, and escape from these kinetic traps is frequently rate-limiting. The preponderance of kinetic traps in RNA folding has obscured more fundamental aspects, such as conformational search and metal ion binding (*1*−*3*).

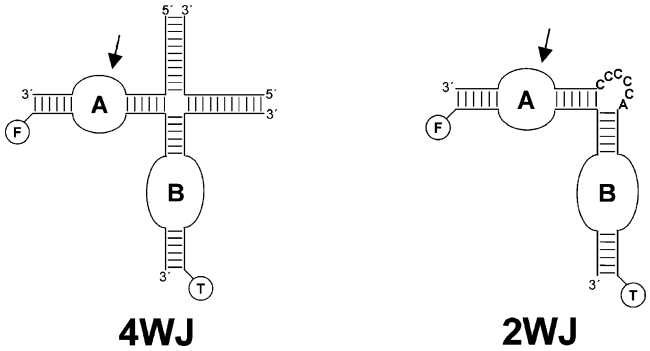

FIGURE 1: Hairpin ribozyme constructs used in the present study. The circles labeled "F" and "T" denote the fluorescein donor and tetramethylrhodamine acceptor, respectively. The arrow indicates the potential cleavage site in each ribozyme.

To elucidate the details of conformational search and metal ion binding in RNA folding, it is useful to employ a small RNA that forms a relatively simple tertiary structure and avoids kinetic traps. The hairpin ribozyme is a small catalytic RNA, comprised of two internal loops and an intervening multihelix junction (Figure 1). To achieve catalytic activity, the ribozyme must fold into a compact conformation that juxtaposes the two loops, facilitating the formation of tertiary hydrogen-bonding interactions between them (*7*−*9*). In the natural form of the hairpin ribozyme, the two loop-carrying duplexes are arranged as two arms of a four-way helical junction (4WJ, Figure 1). However, a minimal ribozyme construct consisting of just the two loop-carrying duplexes

† Supported by a grant from the National Institutes of Health to D.P.M. (Grant GM58873), a fellowship from the Deutsche Forschungsgemeinschaft to G.P., and an EMBO fellowship to D.K.

* To whom correspondence should be addressed. Phone: (858) 784 9870. Fax: (858) 784-9067. E-mail: millar@scripps.edu.

‡ These authors contributed equally to this work.

§ Present address: Department of Experimental Physics IV, University of Bayreuth, 95440 Bayreuth, Germany.

10.1021/bi047772i CCC: $30.25
Published on Web 02/26/2005

(two-way junction (2WJ), Figure 1) is also active in catalysis (*10*).

Because of the large conformational change, the folding and domain docking of the hairpin ribozyme can be conveniently monitored by means of fluorescence resonance energy transfer (FRET)[1] between donor and acceptor probes attached to the ends of the loop-carrying arms. The close physical proximity of the two loops in the folded ribozyme structure was first established by means of steady-state FRET experiments (*11*, *12*). Subsequent time-resolved FRET measurements were used to quantify subpopulations of folded and extended ribozyme conformers and to identify structural elements that contribute to the tertiary structure stability (*9*, *13*, *14*). Recent single-molecule FRET experiments have revealed multiple conformational states of the hairpin ribozyme and detected spontaneous transitions among these (*15*−*17*).

Previous ensemble and single-molecule studies have established that the docking of the hairpin ribozyme loops occurs slowly (*11*, *15*, *16*). In fact, the tertiary structure of the hairpin ribozyme forms almost as slowly as that of much larger ribozymes. This slow docking is especially surprising given recent evidence showing that the two loops are repeatedly brought into close physical proximity by virtue of the conformational dynamics of the four-way helical junction element (*16*, *17*). To investigate the origin of the slow docking, we have conducted a detailed kinetic analysis of hairpin ribozyme folding by means of ensemble stopped-flow FRET measurements. We have investigated the folding kinetics of the natural 4WJ form of the ribozyme, as well as a minimal 2WJ construct, utilizing two different methods to initiate folding. From an analysis of the temperature-dependent docking rates, we have quantified the enthalpic and entropic contributions to the overall activation barrier for each ribozyme construct. In contrast to most previous studies of RNA folding, we find that the slow docking of the hairpin ribozyme is due to an unfavorable entropy change in reaching the transition state for tertiary structure formation. These observations indicate that the ribozyme tertiary structure forms through a slow conformational search. This behavior is observed in both the natural and minimal forms of the ribozyme, indicating that the conformational search is confined to the two loop regions and is largely independent of the overall ribozyme architecture. Our results establish the hairpin ribozyme as a convenient and tractable model system to study this fundamental aspect of RNA tertiary folding.

MATERIALS AND METHODS

RNA Constructs. RNA oligonucleotides were obtained from Dharmacon (Lafayette, CO). Oligonucleotide sequences were 5′-Fl-AAA UAG AGA AGC GAA CCA GAG AAA CAC ACG CA-3′ (strand A), 5′-TMR-UGC GUG GUA CAU UAC CUG GUA CGA GUU GAC-3′ (strand B), 5′-GUC AAC UCG UGG UGG CUU GC-3′ (strand C), 5′-GCA AGC CAC CUC GCdA GUC CUA UUU-3′ (strand D), and 5′-TMR-UGC GUG GUA CAU UAC CUG GUA CCC CCU CGC dAGU CCU AUU U-3′ (strand E). The deoxyadenosine in strands D and E blocked ribozyme cleavage during the fluorescence measurements. All oligonucleotides were deprotected according to the manufacturer's specifications and purified by gel electrophoresis followed by reversed-phase HPLC. 2WJ ribozyme complexes were annealed by mixing 1 μM strand A and 2 μM strand E in annealing buffer (50 mM Tris/HCl, pH 7.5, 100 mM NaCl), followed by incubation at 70° C for 5 min and cooling to ambient temperature. 4WJ ribozyme complexes for Mg-induced folding reactions were annealed by mixing 1 μM strand A and 2 μM each of strands B−D in annealing buffer, followed by heating and cooling as described above. 4WJ ribozyme complexes for substrate-triggered folding reactions were annealed by mixing 1 μM strand A and 2 μM each of strands B and C in annealing buffer, followed by heating and cooling as previously described. Annealed ribozymes were subsequently diluted to a 200 nM donor concentration in standard buffer (50 mM Tris/HCl, pH 7.5, 20 mM NaCl, and 2 mM DTT) and a desired concentration of $MgCl_2$ for substrate-triggered folding reactions.

Folding Kinetics. Folding reactions were conducted in a stopped-flow rapid mixing cell attached to an SLM8100 fluorimeter and monitored in real time by means of fluorescence resonance energy transfer between donor (Fl) and acceptor (TMR) dyes attached to the ends of the arms carrying loops A and B, respectively. Magnesium-induced folding of 2WJ or 4WJ ribozymes was initiated by rapid mixing of the respective ribozyme (final donor concentration 100 nM) with a desired concentration of $MgCl_2$ (final concentration of 2−20 mM) in standard buffer. Substrate-induced folding reactions were initiated by rapid mixing of the 4WJ ribozyme in standard buffer (lacking strand D, final donor concentration 100 nM) with strand D (final concentration 1 μM) and a desired final concentration of $MgCl_2$ in standard buffer. Strand D was heated to 70°C and slowly cooled to room temperature prior to being mixed with the ribozyme.

In all folding reactions, the fluorescein donor was excited at 495 nm (2 nm band-pass) and the fluorescence of the donor and that of the acceptor were separately monitored over time using appropriate filters (530 nm band-pass filter for Fl, OG590 long-pass filter for TMR). The emission transients of the donor or acceptor were fitted using double-exponential functions to obtain the folding rates, $k_{obs,1}$ and $k_{obs,2}$. The temperature dependence of the folding rates was analyzed using Eyring transition-state theory. Plots of $\ln(k_{obs}/T)$ versus $1/T$ were fit according to eq 1 to obtain values for the

$$\ln\left(\frac{k_{obs}}{T}\right) = \frac{-\Delta H^{\ddagger}_{app}}{RT} + \frac{\Delta S^{\ddagger}_{app}}{R} + \ln\frac{k_b}{h} \qquad (1)$$

apparent activation enthalpy ($\Delta H^{\ddagger}_{app}$) and entropy ($\Delta S^{\ddagger}_{app}$). In eq 1, T is the absolute temperature, R is the general gas constant (8.314 J mol^{-1} K^{-1}), k_b is the Boltzmann constant (1.38×10^{-23} J K^{-1}), and h is Planck's constant (6.626×10^{-34} J s).

RESULTS

Kinetics of Hairpin Ribozyme Folding Monitored by Stopped-Flow FRET. To monitor the tertiary folding of the hairpin ribozyme, we attached donor (Fl) and acceptor

[1] Abbreviations: Fl, fluorescein; TMR, tetramethylrhodamine; FRET, fluorescence resonance energy transfer; trFRET, time-resolved fluorescence resonance energy transfer.

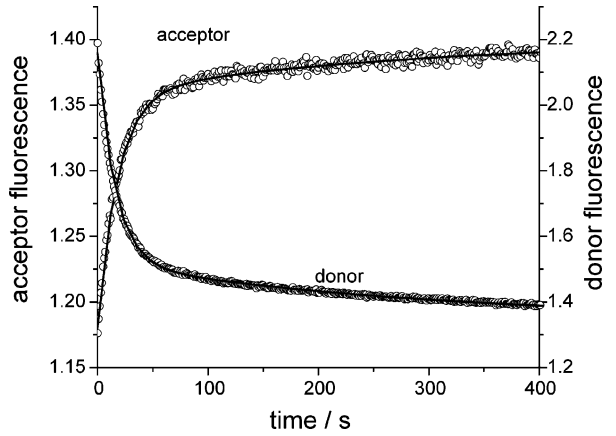

FIGURE 2: Donor and acceptor emission transients during substrate-induced folding of the 4WJ ribozyme. Preannealed ribozyme (200 nM, lacking the pseudosubstrate strand) in 50 mM Tris/HCl, pH 7.5, 20 mM NaCl, 2 mM DTT, 12 mM $MgCl_2$ was rapidly mixed with 2 μM pseudosubstrate in the same buffer, and the donor and acceptor emissions were monitored over time using 530 nm band-pass and 590 nm long-pass filters, respectively. The solid lines are double-exponential fits to the emission transients. The folding rates obtained from fitting the donor emission are $k_{obs,1} = (6.27 \pm 0.04) \times 10^{-2}$ s^{-1} and $k_{obs,2} = (3.51 \pm 0.06) \times 10^{-3}$ s^{-1}, and the corresponding fractional amplitudes are 0.78 ± 0.01 and 0.22 ± 0.01, respectively. The rates obtained from the fit to the acceptor emission are $k_{obs,1} = (5.47 \pm 0.08) \times 10^{-2}$ s^{-1} and $k_{obs,2} = (3.68 \pm 0.17) \times 10^{-3}$ s^{-1}, with fractional amplitudes of 0.81 ± 0.01 and 0.19 ± 0.01, respectively.

(TMR) dyes to the ends of the arms carrying loops A and B, respectively (Figure 1). Since the two loops are brought into close proximity during folding, the process can be monitored in real time by observing changes in the efficiency of FRET between the donor and acceptor. We initially studied the natural form of the ribozyme, in which the loop-containing duplexes are arranged as two arms of a 4WJ (Figure 1). The 4WJ ribozyme was assembled from four oligonucleotides (Figure 1). Two different methods were used to initiate folding. In one method, all four strands were annealed in the absence of divalent cations, resulting in an extended conformation of the ribozyme with a low FRET efficiency between the labeled arms (*11*, *12*). Folding was then initiated by rapidly mixing the ribozyme with $MgCl_2$. Previous studies have shown that Mg^{2+} promotes folding of the ribozyme and stabilizes the resulting tertiary structure (*11*, *12*). In the other method, the ribozyme was annealed in the absence of the substrate strand but in the presence of $MgCl_2$, resulting in a three-stranded complex lacking loop A. The remaining strand (termed the pseudosubstrate) containing the potential cleavage site (blocked by a 2′-deoxy modification) was then rapidly mixed with this complex, resulting in the formation of loop A and initiating the folding of the complete 4WJ ribozyme. For both methods, the mixing was performed in a stopped-flow mixing cell attached to a spectrofluorimeter (~2 ms mixing time). The emissions of both the donor and acceptor were separately monitored over time after mixing.

Figure 2 shows typical emission transients from a substrate-induced folding reaction. Following addition of the pseudosubstrate strand, the donor emission decreased slowly over time while the acceptor showed a corresponding increase. Moreover, the rate of the donor fluorescence decrease matched the rate of the acceptor increase (see below). These observations confirm that both emission transients were monitoring a shortening of the donor−acceptor distance as the 4WJ ribozyme folded to a final conformation in which loops A and B were in close physical proximity. Similar behavior was observed in Mg-induced folding reactions. To extract the rate of folding, we attempted to fit single-exponential curves to the donor or acceptor emission transients, but the resulting fits were poor. However, good fits were obtained by using a sum of two exponential functions (Figure 2). Moreover, the individual folding rates obtained from either the donor or acceptor emission were in good agreement. The consistency of the donor and acceptor rates was observed under all experimental conditions tested and for both methods used to induced folding of the ribozyme.

In addition to the emission changes observed following mixing of the 4WJ ribozyme with Mg^{2+} or the pseudosubstrate strand, a modest increase in FRET efficiency occurred within the ~100 ms integration time (data not shown). This rapid phase accounts for ~20% of the total signal change for either donor or acceptor. We also observed this rapid FRET change during Mg-induced folding of a 4WJ construct lacking loop A (the 3′ portion of strand D was complementary to strand A, eliminating loop A). Since the single-loop construct was incapable of forming a docked tertiary structure, the initial FRET change was attributed to a partial folding step prior to docking (see the Discussion).

To assess the influence of the multihelix junction on ribozyme folding behavior, we also examined a minimal ribozyme construct consisting of just the two loop-containing duplexes joined by a single-stranded AC_5 linker (Figure 1). This construct is referred to as a 2WJ ribozyme. Since the substrate portion was covalently joined to the remainder of the ribozyme, folding could only be induced through the addition of Mg^{2+} ions to the ribozyme. Interestingly, there was no change in the emission of the donor or acceptor during the mixing time, although the slow emission changes following mixing were qualitatively similar to those observed for Mg^{2+}-induced folding of the 4WJ ribozyme. The emission transients of either donor or acceptor required two exponentials for the best fit, as before.

Dependence of Folding Rates on Magnesium Ion Concentration. To confirm the existence of two distinct kinetic phases, we investigated the folding kinetics of both 2WJ and 4WJ hairpin ribozyme constructs across a range of final Mg^{2+} concentrations, from 2 to 20 mM (at a temperature of 24 °C). For Mg^{2+}-induced folding of the 2WJ or 4WJ ribozymes, the respective ribozyme was rapidly mixed with different final concentrations of $MgCl_2$. For substrate-triggered folding of the 4WJ ribozyme, the three-strand ribozyme complex was annealed in the presence of different Mg^{2+} concentrations before being rapidly mixed with the pseudosubstrate strand. Two distinct relaxation rates were observed across the entire Mg^{2+} concentration range. Figure 3 presents the individual relaxation rates recovered from the double-exponential fits at each Mg^{2+} concentration. As is readily evident from Figure 3, both relaxation rates exhibit an approximate linear dependence on the Mg^{2+} concentration, regardless of the ribozyme construct or the method used to induce folding. The Mg^{2+} ions may accelerate folding of the RNA chain into a compact structure by increased charge

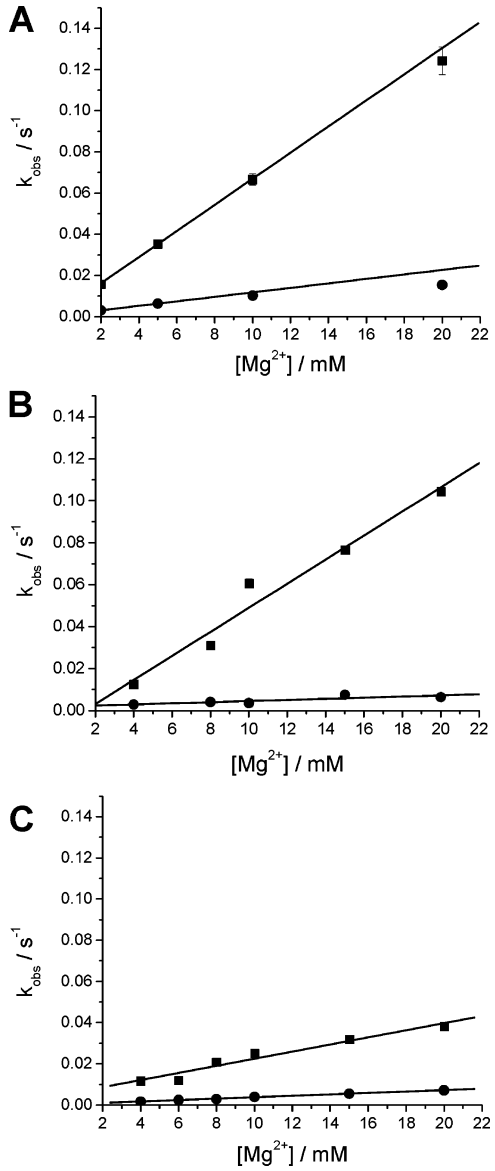

FIGURE 3: Dependence of individual ribozyme folding rates on Mg^{2+} concentration. (A) Mg^{2+}-induced folding of the 2WJ ribozyme. Folding was initiated by addition of the indicated final concentration of $MgCl_2$ to the ribozyme. (B) Substrate-induced folding of the 4WJ ribozyme. Folding was initiated by addition of the pseudosubstrate strand to the ribozyme in the presence of the indicated concentration of $MgCl_2$. (C) Mg^{2+}-induced folding of the 4WJ ribozyme. Folding was initiated by addition of the indicated final concentration of $MgCl_2$ to the ribozyme. In all cases, individual folding rates $k_{obs,1}$ (squares) and $k_{obs,2}$ (circles) were obtained from double-exponential fits to the transient donor emission. The lines are linear regression best fits to the data.

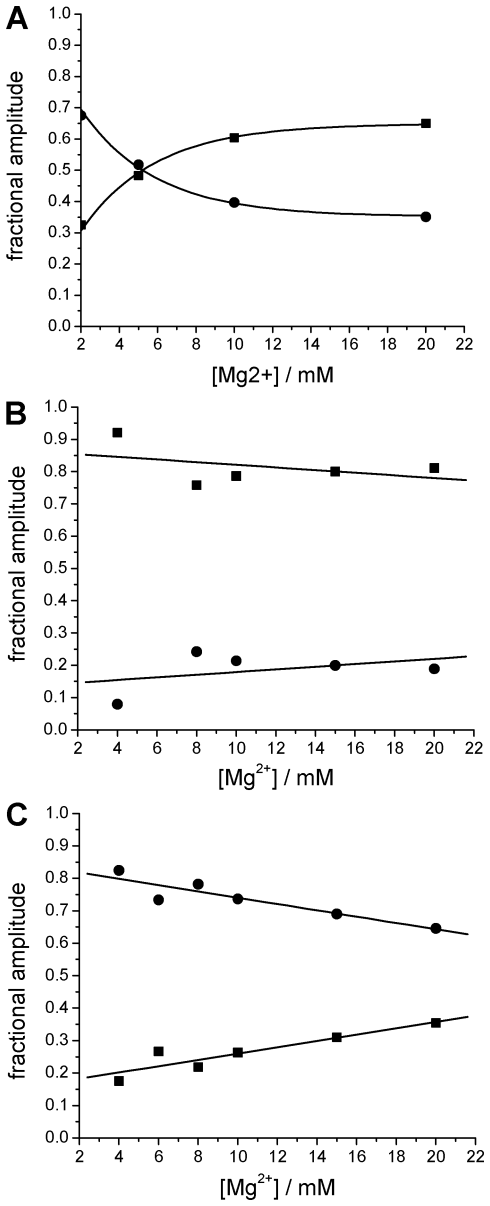

FIGURE 4: Fractional amplitudes of individual kinetic phases at different Mg^{2+} concentrations. (A) Mg^{2+}-induced folding of the 2WJ ribozyme. Folding was initiated by addition of the indicated final concentration of $MgCl_2$ to the ribozyme. (B) Substrate-induced folding of the 4WJ ribozyme. Folding was initiated by addition of the pseudosubstrate strand to the ribozyme in the presence of the indicated concentration of $MgCl_2$. (C) Mg^{2+}-induced folding of the 4WJ ribozyme. Folding was initiated by addition of the indicated final concentration of $MgCl_2$ to the ribozyme. In all cases, the fractional amplitudes associated with relaxation rates $k_{obs,1}$ (squares) and $k_{obs,2}$ (circles) were obtained from double-exponential fits to the transient donor emission at the respective Mg^{2+} concentration. The corresponding rates are presented in Figure 3.

shielding of phosphate groups. Overall, the correspondence between the folding rates observed for the different ribozyme constructs and triggering methods strongly suggests that two distinct folding pathways are traversed in each case.

Despite the similarities in the individual relaxation rates, the amplitudes of the two kinetic phases were different for 2WJ and 4WJ ribozyme constructs. For Mg^{2+}-induced folding of the 2WJ, the amplitude of the fast kinetic phase increased somewhat with Mg^{2+} concentration, while the amplitude of the slow phase decreased correspondingly (Figure 4A). In the case of Mg^{2+}-induced folding of the 4WJ ribozyme, the amplitudes of the fast and slow kinetic phases were roughly independent of Mg^{2+} concentration and the slow kinetic phase was dominant (Figure 4C). However, when folding of the 4WJ ribozyme was initiated by pseudosubstrate binding, the fast phase was dominant at all Mg^{2+} concentrations tested (Figure 4B).

Temperature Dependence of Folding Kinetics. Stopped-flow FRET measurements were carried out for the 2WJ and 4WJ ribozymes across a range of temperatures from 8 to 32 °C, using both substrate- and Mg^{2+}-triggering to initiate folding of the 4WJ ribozyme. Biphasic relaxation behavior was observed in all cases. Both relaxation rates were largely

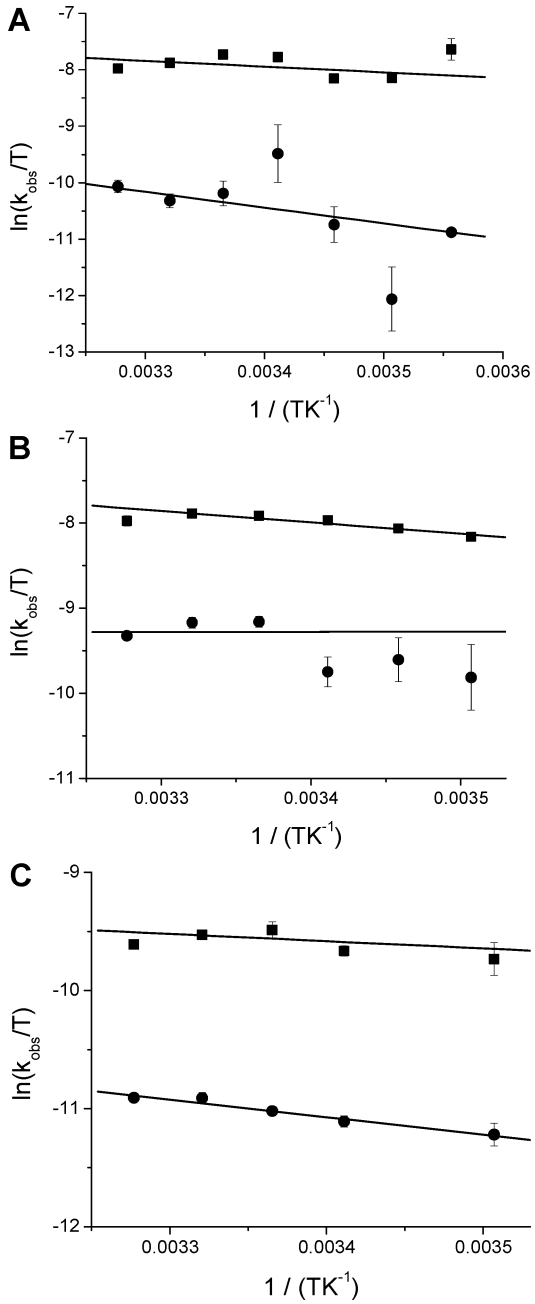

FIGURE 5: Eyring plots for tertiary structure formation in the hairpin ribozyme. (A) 2WJ ribozyme folding initiated by mixing with 12 mM $MgCl_2$. (B) 4WJ ribozyme folding initiated by addition of the pseudosubstrate strand in the presence of 12 mM $MgCl_2$. (C) 4WJ ribozyme folding initiated by mixing with 12 mM $MgCl_2$. In all cases, data points are shown for both $k_{obs,1}$ (squares) and $k_{obs,2}$ (circles). The solid lines are best fits to the Eyring equation (see the text for details).

independent of temperature, regardless of the ribozyme construct or the method used to initiate folding. The results are presented in the form of Eyring plots in Figure 5. The slope of the Eyring plot is related to the apparent activation enthalpy, $\Delta H^{\ddagger}_{app}$, while the intercept yields the apparent activation entropy, $\Delta S^{\ddagger}_{app}$. As expected from the shallow slopes of the Eyring plots, the apparent activation enthalpy is small in all cases (Table 1). The intercepts of the Eyring plots indicate that the activation entropy has a significant negative value in all cases. Accordingly, the entropic component, $-T\Delta S^{\ddagger}_{app}$, makes the dominant contribution to the overall activation barrier for docking in all cases (Table 1). This large entropic barrier is principally responsible for the slow docking of both the 2WJ and 4WJ ribozymes.

Table 1: Apparent Activation Parameters for Hairpin Ribozyme Folding[a]

ribozyme construct	triggering method	rate	$\Delta H^{\ddagger}_{app}$ (kJ mol^{-1})	$-T\Delta S^{\ddagger}_{app}$[b] (kJ mol^{-1})
2WJ	Mg^{2+}	$k_{obs,1}$	8 ± 7	70 ± 7
		$k_{obs,2}$	23 ± 4	61 ± 4
4WJ	Mg^{2+}	$k_{obs,1}$	5 ± 6	77 ± 6
		$k_{obs,2}$	12 ± 2	74 ± 2
4WJ	substrate	$k_{obs,1}$	11 ± 1	67 ± 1
		$k_{obs,2}$	0 ± 11	82 ± 11

[a] Folding reactions contained 12 mM $MgCl_2$. [b] Calculated at 298 K.

DISCUSSION

Hairpin Ribozyme Folding Pathways. We have monitored the folding kinetics of the hairpin ribozyme by measurements of FRET between donor and acceptor dyes attached to the arms carrying loops A and B. Using either the natural 4WJ form of the ribozyme or a minimal 2WJ construct, we observed two distinct kinetic phases as the ribozyme folded from an initial extended conformation to a final conformation with loops A and B in close proximity. These two kinetic phases were observed under all experimental conditions tested and when two different methods were used to induce folding of the 4WJ ribozyme. Hence, the existence of at least two kinetic phases appears to be a general property of hairpin ribozyme folding.

In principle, the two kinetic phases could arise from two parallel folding pathways or from a sequential pathway involving a discrete folding intermediate. Our stopped-flow FRET data do not distinguish between these two possibilities. However, previous single-molecule FRET studies of the 2WJ form of the ribozyme have revealed heterogeneous folding behavior, attributed to four distinct species with different undocking rates (*15*). Significantly, these species do not appear to interconvert during the time scale of folding. Since our relaxation rates are a composite of both the docking and undocking rates, these ribozyme subpopulations might be distinguishable in our ensemble stopped-flow experiments. To effect a direct comparison, the docking and undocking rates reported in the single-molecule FRET study (performed at 22 °C in the presence of 12 mM $MgCl_2$) were summed to yield the relaxation rates that would be expected in our stopped-flow experiments: the resulting values are 0.013, 0.061, 0.5, and 3 s^{-1} (*15*). Interestingly, the first two rates closely match the relaxation rates found here for the 2WJ ribozyme under similar conditions ($k_{obs,2} = 0.010 \pm 0.007$ s^{-1} and $k_{obs,1} = 0.067 \pm 0.003$ s^{-1} at 20 °C and in the presence of 10 mM $MgCl_2$, Figure 3A). Hence, in accord with the single-molecule FRET results, we attribute the biphasic relaxation kinetics to two distinct ribozyme species that fold along parallel pathways and that undock at different rates (Figure 6A). These species may differ in the number of tertiary hydrogen bonds formed in the docked state, as has been suggested previously for the 2WJ ribozyme (*15*). The two ribozyme species with the fastest undocking rates in the single-molecule FRET studies are not manifested in our ensemble stopped-flow experiments, presumably because they are only fleetingly populated.

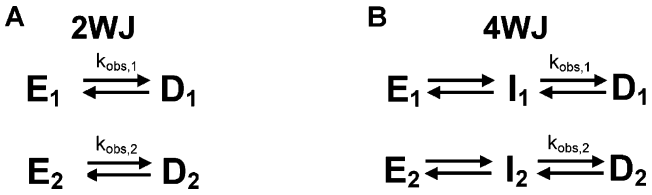

FIGURE 6: Models for the folding pathways of the 2WJ and 4WJ hairpin ribozymes. (A) Folding pathway of the minimal 2WJ ribozyme. E_1, E_2 and D_1, D_2 denote noninterconverting subpopulations of extended and docked ribozyme conformers, respectively, distinguished by different relaxation rates, $k_{obs,1}$ and $k_{obs,2}$ ($k_{obs,1} > k_{obs,2}$). Previous single-molecule FRET studies of the 2WJ ribozyme suggest that the difference in relaxation rates arises primarily from distinct undocking rates of D_1 and D_2 (*15*). (B) Folding of the natural 4WJ ribozyme. E_1, E_2 and D_1, D_2 are defined as in (A). Additionally, I_1 and I_2 represent intermediates in each folding pathway. See the text for details.

In view of the similar kinetic behavior of both forms of the ribozyme, we propose that two parallel folding pathways with different undocking rates are also a property of the 4WJ ribozyme. In addition to the two relaxation rates, we also observed a rapid FRET change during the initial folding of the 4WJ ribozyme that was complete within the 100 ms integration time. In principle, this may reflect a third kinetic pathway characterized by very fast docking and/or undocking transitions. However, the fast FRET change was also observed in a 4WJ ribozyme construct lacking loop A, which is incapable of forming a docked tertiary structure. Hence, we attribute the initial FRET change to a partial folding of the 4WJ ribozyme that brings the loop-carrying arms into close proximity without the formation of tertiary docking interactions. Our recent single-pair FRET studies of a single-loop 4WJ ribozyme indicate that this folding occurs on the submillisecond time scale (*17*). Since the initial folding is fast, the subsequent docking of loops A and B presumably occurs from this compact state, although our stopped-flow data do not formally prove that this species actually lies on the folding pathway. However, a recent single-molecule FRET study of the 4WJ ribozyme has revealed the existence of a discrete folding intermediate (*16*). Hence, we tentatively assign the initial FRET change to the formation of a folding intermediate. The proposed docking pathway of the 4WJ ribozyme is shown in Figure 6B.

In the stopped-flow measurements of 4WJ ribozyme folding, we observed two relaxation rates regardless of the method used to induce the folding. Interestingly, the relative amplitudes of the two kinetic phases were quite different for substrate-induced and Mg-induced reactions (Figure 4), suggesting that the partitioning between the two folding pathways in Figure 6B was dependent on the method used to anneal the ribozyme and to induce folding. Substrate-induced folding strongly favored the faster relaxation channel, characterized by a faster rate of unfolding from the docked tertiary structure. For these reactions, the ribozyme was first annealed in the absence of the substrate strand and a pseudosubstrate strand was then added to initiate folding. Since loop A is not formed until the pseudosubstrate is added, it is possible that the loop adopts an aberrant structure immediately after the substrate strand is bound and is incapable of forming a complete tertiary interaction network with loop B, resulting in a faster rate of undocking.

Origin of Slow Tertiary Structure Formation. It is surprising that the tertiary structure of the hairpin ribozyme forms so slowly given the apparent simplicity of the docking process. In fact, the folding rate is comparable to that of much larger ribozymes that form more complex tertiary structures (*1*−*3*). Slow folding of RNA to the native state is most often the result of alternative secondary structures or non-native tertiary structures that act as kinetic traps during folding (*1*). Because the escape from these traps is usually rate-limiting and requires the disruption of the non-native structures, the folding rate is strongly temperature-dependent and the activation enthalpy for folding is correspondingly high. Examples of slowly folding RNAs that encounter kinetic traps include the P3 domain of the *Tetrahymena* ribozyme ($\Delta H^{\ddagger} = 92$ kJ mol^{-1}; *18*), *Bacillus subtilis* P RNA ($\Delta H^{\ddagger} = 208$ kJ mol^{-1}; *19*), and tRNAs from various organisms ($\Delta H^{\ddagger} = 120-240$ kJ mol^{-1}; *20*, *21*).

Surprisingly, we find that the folding kinetics of either the 2WJ or 4WJ form of the hairpin ribozyme are essentially independent of temperature (Figure 5). Moreover, the apparent activation enthalpies associated with either of the two relaxation rates are relatively small in all cases (Table 1). Since the relaxation rates measured in our stopped-flow experiments are actually composite rates, equal to the sum of the elementary docking and undocking rates, the apparent lack of temperature dependence could arise from compensatory changes of these underlying rates. For example, the docking and undocking rates may vary with temperature in equal and opposite ways, such that their sum remains approximately constant. If so, the equilibrium constant for docking, equal to the ratio of these rates, would be strongly temperature-dependent. In fact, the equilibrium constants for docking of both 2WJ and 4WJ ribozymes are constant across the range of temperatures examined here (*14*). Hence, the intrinsic docking and undocking rates must also be independent of temperature.

The slow folding rate and lack of significant temperature dependence suggest that the tertiary structure of the hairpin ribozyme is formed through a slow conformational search. Consistent with this, the entropic contribution to the overall activation barrier is much larger than the enthalpic term, regardless of which relaxation rate is considered (Table 1). Moreover, the magnitude of the entropic barrier is similar in both forms of the ribozyme, suggesting that the conformational search process is primarily associated with the two loop regions and is unaffected by the presence or absence of the other junction arms. The X-ray crystal structure of the hairpin ribozyme in its docked conformation reveals many hydrogen-bonding interactions at the interface between loops A and B (*7*). A ribose zipper network connects two nucleotides from loop A (A_{10} and G_{11}) to two nucleotides within loop B (A_{24} and C_{25}), the G_{+1} base from loop A forms a Watson−Crick base pair with C_{25} from loop B, and the 2′-hydroxyl of G_{+1} forms an additional hydrogen bond with G_{36} from loop B. Additionally, U_{42} from loop B forms hydrogen bonds with G_{11} and U_{12} from loop A. Notably, many of the tertiary interactions involve nucleotides that are far apart in the primary sequence and secondary structure. The need to juxtapose distant nucleotides necessarily involves a loss of conformational entropy, accounting for the unfavorable activation entropy for tertiary structure formation. This is similar to the situation in protein folding where juxtaposition of widely separated amino acids results in slow folding kinetics (*22*).

Other notable features of the docked ribozyme structure are the extrahelical conformations adopted by the nucleotides G_{+1} and U_{42} (*7*). In contrast, both bases are stacked within their respective loops in the structures of the isolated loop A (*23*) and loop B (*24*) domains. Hence, rearrangements of the two loops and flipping of G_{+1} and U_{42} from intra- to extrahelical conformations may also contribute to the conformational search. However, simple base flipping is not sufficient to explain the slow docking kinetics. In fact, flipping of G_{+1} and U_{42} must be spatially and temporally coincident with the presentation of their complementary interaction partners for tertiary interactions to form. These requirements, together with the need to juxtapose distant nucleotides in the primary sequence, are probably the key determinants of the conformational search process.

Generality of Conformational Search in RNA Tertiary Structure Formation. Conformational search is recognized as a fundamental aspect of RNA tertiary folding (*3*). However, the strong propensity of RNA molecules to populate alternative secondary or tertiary structures that act as kinetic traps during folding has obscured this key mechanistic feature in most studies of RNA folding. It was suggested previously that the slow tertiary folding of the hairpin ribozyme might be due to a conformational search process (*11*). However, the results of the present study provide the first direct experimental evidence for a conformational search mechanism in the hairpin ribozyme. As far as we are aware, there are only two other reported examples of RNA molecules that attain their tertiary structure through a conformational search, the 303-nt bI5 group I intron core domain (*25*) and the D135 ribozyme derived from the ai5γ group II intron (*26*). Both of these RNAs are much larger than the hairpin ribozyme. In the case of the bI5 group I intron core domain, the folding rate was measured as a function of temperature, revealing folding behavior similar to that of the hairpin ribozyme. The RNA folds slowly and the rate is independent of temperature, indicating the activation enthalpy is negligible (*25*). Hence, folding of the relatively small hairpin ribozyme may capture general mechanistic features of RNA tertiary folding. Given the relative ease of synthesis and site-specific modification, the ability to fold independently, and the availability of three-dimensional structural data on the folded and unfolded states, the hairpin ribozyme is an attractive and tractable model system for detailed investigations of fundamental mechanistic features of RNA folding such as conformational search and metal ion binding. The kinetic analysis described here can be applied to hairpin ribozyme variants containing specific nucleotide modifications to identify the determinants of the conformational search.

REFERENCES

1. Treiber, D. K., and Williamson, J. R. (1999) Exposing the kinetic traps in RNA folding, *Curr. Opin. Struct. Biol. 9*, 339−345.
2. Treiber, D. K., and Williamson, J. R. (2001) Beyond kinetic traps in RNA folding, *Curr. Opin. Struct. Biol. 11*, 309−314.
3. Sosnick, T. R., and Pan, T. (2003) RNA folding: models and perspectives, *Curr. Opin. Struct. Biol. 13*, 309−316.
4. Russell, R., Millett, I. S., Doniach, S., and Herschlag, D. (2000) Small-angle X-ray scattering reveals a compact intermediate in RNA folding, *Nat. Struct. Biol. 7*, 367−70.
5. Russell, R., Millett, I. S., Tate, M. W., Kwok, L. W., Nakatani, B., Gruner, S. M., Mochrie, S. G., Pande, V., Doniach, S., and Herschlag, D. (2002a) Rapid compaction during RNA folding, *Proc. Natl. Acad. Sci. U.S.A. 99*, 4266−71.
6. Russell, R., Zhuang, X., Babcock, H. P., Millett, I. S., Doniach, S., Chu, S., and Herschlag, D. (2002b) Exploring the folding landscape of a structured RNA, *Proc. Natl. Acad. Sci. U.S.A. 99*, 155−160.
7. Rupert, P. B., and Ferre-D'Amare, A. R. (2001) Crystal structure of a hairpin ribozyme-inhibitor complex with implications for catalysis, *Nature 410*, 780−786.
8. Klostermeier, D., and Millar, D. P. (2002) Tertiary structure stability of the hairpin ribozyme in its natural and minimal forms: Different energetic contributions from a ribose zipper motif, *Biochemistry 40*, 11211−11218 (2001).
9. Klostermeier, D., and Millar, D. P. (2003) Energetics of hydrogen bond networks in RNA: Hydrogen bonds surrounding G_{+1} and U_{42} are the major determinants for tertiary structure stability of the hairpin ribozyme, *Biochemistry 41*, 14095−14102.
10. Hampel, A., and Tritz, R. (1989) RNA catalytic properties of the minimum (−)sTRSV sequence, *Biochemistry 28*, 4929−4933.
11. Walter, N. G., Hampel, K. J., Brown, K. M., and Burke, J. M. (1998) Tertiary structure formation in the hairpin ribozyme monitored by fluorescence resonance energy transfer, *EMBO J. 17*, 2378−2391.
12. Murchie, A. I. H., Thompson, J. B., Walter, F., and Lilley, D. M. J. (1998) Folding of the hairpin ribozyme in its natural conformation achieves close physical proximity of the loops, *Mol. Cell 1*, 873−881.
13. Walter, N. G., Burke, J. M., and Millar, D. P. (1999) Stability of hairpin ribozyme tertiary structure is governed by the interdomain junction, *Nat. Struct. Biol. 6*, 544−549.
14. Klostermeier, D., and Millar, D. P. (2000) Helical junctions as determinants for RNA folding: origin of tertiary structure stability of the hairpin ribozyme, *Biochemistry 39*, 12970−12978.
15. Zhuang, X., Kim, H., Pereira, M. J., Babcock, H. P., Walter, N. G., and Chu, S. (2002) Correlating structural dynamics and function in single ribozyme molecules, *Science 296*, 1473−1476.
16. Tan, E., Wilson, T. J., Nahas, M. K., Clegg, R. M., Lilley. D. M. J., and Ha, T. (2003) A four-way junction accelerates hairpin ribozyme folding via a discrete folding intermediate, *Proc. Natl. Acad. Sci. U.S.A. 100*, 9308−9313.
17. Pljevaljcic, G., Millar, D. P., and Deniz, A. A. (2004) Freely-diffusing single hairpin ribozymes provide insights into the role of secondary structure and partially-folded states in RNA folding, *Biophys. J. 87*, 457−467.
18. Rook, M. S, Treiber, D. K., and Williamson, J. R. (1998) Fast folding mutants of the Tetrahymena group I ribozyme reveal a rugged folding energy landscape, *J. Mol. Biol. 281*, 609−20.
19. Pan, T., and Sosnick, T. R. (1997) Intermediates and kinetic traps in the folding of a large ribozyme revealed by CD and UV spectroscopies and catalytic activity, *Nat. Struct. Biol. 14*, 931−938.
20. Cole, P. E., Yang, S. K., and Crothers, D. M. (1972) Conformational changes of transfer ribonucleic acid. Equilibrium phase diagrams, *Biochemistry 11*, 4358−4368.
21. Lynch, D. C., and Schimmel, P. R. (1974) Cooperative binding of magnesium to transfer ribonucleic acid studied by a fluorescent probe, *Biochemistry 13*, 1841−1852.
22. Plaxco, K. W., Simons, K. T., and Baker, D. (1998) Contact order, transition state placement and the refolding rates of single domain proteins, *J. Mol. Biol. 277*, 985−994.
23. Cai, Z., and Tinoco, I. (1996) Solution structure of loop A from the hairpin ribozyme from tobacco ringspot virus satellite, *Biochemistry 35*, 6026−6036.
24. Butcher, S. E., Allain, F. H. T., and Feigon, J. (1999) Solution structure of the loop B domain from the hairpin ribozyme, *Nat. Struct. Biol. 6*, 212−216.
25. Buchmueller, K. L., Webb, A. E., Richardson D. A., and Weeks, K. M. (2000) A collapsed non-native RNA folding state, *Nat. Struct. Biol. 7*, 362−366.
26. Swisher, J. F., Su, L. J., Brenowitz, M., Anderson, V., and Pyle, A. M. (2002) Productive folding to the native state by a group II intron ribozyme, *J. Mol. Biol. 315*, 297−310.

BI047772I